Nanomedicine Hot Paper

DOI: 10.1002/anie.201404766

Development of Multinuclear Polymeric Nanoparticles as Robust Protein Nanocarriers**

*Jun Wu, Nazila Kamaly, Jinjun Shi, Lili Zhao, Zeyu Xiao, Geoffrey Hollett, Rohit John, Shaunak Ray, Xiaoyang Xu, Xueqing Zhang, Philip W. Kantoff, and Omid C. Farokhzad**

Abstract: *One limitation of current biodegradable polymeric nanoparticles is their inability to effectively encapsulate and sustainably release proteins while maintaining protein bioactivity. Here we report the engineering of PLGA–polycation nanoparticles with a core–shell structure that act as a robust vector for the encapsulation and delivery of proteins and peptides. The optimized nanoparticles can load high amounts of proteins (>20% of nanoparticles by weight) in aqueous solution without organic solvents through electrostatic interactions by simple mixing, thereby forming nanospheres in seconds with diameters <200 nm. The relationship between nanosphere size, surface charge, PLGA–polycation composition, and protein loading is also investigated. The stable nanosphere complexes contain multiple PLGA–polycation nanoparticles, surrounded by large amounts of protein. This study highlights a novel strategy for the delivery of proteins and other relevant molecules.*

Since the 1970s, protein therapy has become a promising strategy for the effective treatment of cancers, diabetes, cardiovascular diseases, and many other disorders.[1–6] However, the safe and effective delivery of proteins to the desired disease locations or intracellular sites remains a major challenge because of the intrinsic properties of most proteins, such as high molecular weight (MW), surface charges, and vulnerable tertiary structures.[2] Thus, specific and robust delivery vehicles are needed to facilitate the loading, delivery, and controlled release of proteins.

Numerous protein carrier platforms have been developed for better therapeutic performance. For example, microspheres[7] and hydrogels[3,8] have been utilized to solve the sustained-release issue. However, these systems have limited applications for intracellular protein delivery because of their large size. Other systems including liposomes,[9] polymer conjugates,[10] nanotubes,[11] nanogels,[12] and nanoparticles (NPs)[4,6] are being extensively investigated for effective intracellular delivery. Among them, biodegradable polymeric NPs have aroused great interest as potentially robust protein carriers as a result of their biocompatibility, biodegradability, amenability to formulation, and capability with intracellular and systemic delivery.[2,13–15] Nevertheless, the major types of proteins and protein analogues are negatively charged and have complicated, sensitive, and fragile 3D structures and sizes ranging from 2–15 nm. Thus, the currently available polymeric NP platforms require further optimization to load and encapsulate proteins with high efficiency and release them in a sustained manner while maintaining bioactivity.[2]

For effective protein delivery, the ideal polymeric NP platform should show: 1) high protein loading (low NP mass to achieve therapeutic dose); 2) "green" protein encapsulation: little or no organic solvents used to prevent protein denaturation; 3) minimal contact with carriers to avoid the low local pH value caused by polymer degradation;[16,17] and 4) sustainable and controllable protein release with low initial burst. Inspired by the electrostatic interactions between polyelectrolytes, we hypothesized that an NP system with very strong cationic moieties might be ideal to load and release a large quantity of proteins in a safe and controllable manner. A novel protein loading strategy was developed that was based on very strong cationic NPs to physically adsorb proteins to form a new NP/protein complex nanosphere platform in aqueous solution (Figure 1).

To this end, a polymeric NP platform with a cationic shell was first developed from the diblock copolymer of poly(lac-

[*] Dr. J. Wu, Dr. N. Kamaly, Dr. J. Shi, L. Zhao, Dr. Z. Xiao, G. Hollett, R. John, S. Ray, Dr. X. Xu, Dr. X. Zhang, Prof. O. C. Farokhzad
Laboratory of Nanomedicine and Biomaterials, Department of Anesthesiology, Brigham and Women's Hospital
Harvard Medical School, Boston, MA 02115 (USA)
E-mail: ofarokhzad@zeus.bwh.harvard.edu
Dr. J. Wu, Dr. N. Kamaly, Dr. Z. Xiao, Dr. X. Xu, Prof. O. C. Farokhzad
MIT-Harvard Center for Cancer Nanotechnology Excellence
Massachusetts Institute of Technology
Cambridge, MA 02139 (USA)
Prof. O. C. Farokhzad
King Abdulaziz University, Jeddah 22254 (Saudi Arabia)
L. Zhao
School of Life Science, Nanjing University
Nanjing, Jiangsu, 210093 (P.R. China)
Prof. P. W. Kantoff
Lank Center for Genitourinary Oncology, Danan-Farber Cancer Institute, Harvard Medical School, Boston, MA 02115 (USA)

[**] This research was supported by the National Institutes of Health under grant numbers CA151884, HSSN268201000045C, and EB015419 as well as the David Koch-Prostate Cancer Foundation Program in Cancer Nanotherapeutics, Movember Challenge Award from Prostate Cancer Foundation and the National Research Foundation of Korea K1A1A2048701. O.C.F. has financial interest in BIND Therapeutics, Selecta Biosciences, and Blend Therapeutics, biopharmaceutical companies that are developing therapeutic nanoparticles. J.S. acknowledges the financial support from the NCI R00A160350 and PCF Young Investigator Award. X.X. acknowledges the financial support from the NIH National Research Service Award (NRSA) 1F32CA168163-03.

Supporting information for this article is available on the WWW under http://dx.doi.org/10.1002/anie.201404766.

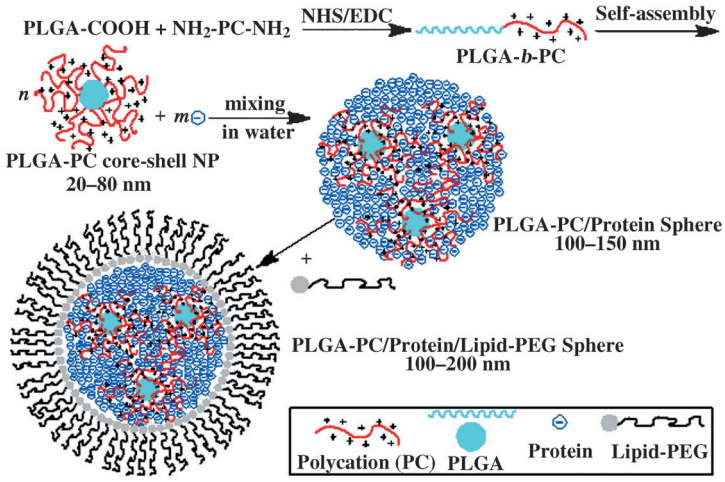

Figure 1. Illustration of the synthesis of PLGA-*b*-polycation (PC) copolymer, PLGA–PC NP, PLGA–PC/protein NP, PLGA–PC/protein/lipid–PEG NP, and the multinuclear structure of the NPs. EDC = *N*′-(3-dimethylaminopropyl)-*N*-ethylcarbodiimide, NHS = *N*-hydroxysuccinimide.

tide-*co*-glycolic acid) (PLGA) and L-arginine-based polycation (PC; Figures 1 and 2). PLGA-based NPs have been widely utilized as a result of their unique biocompatibility, biodegradability, small particle size, and high drug-loading capacity.[18–20] During formulation, the hydrophobic PLGA segments form a solid inner core and limit the NP to a small nanosize, while the hydrophilic and water-soluble PC portion forms the outer shell, thereby creating a very strong electrical field for protein adsorption (loading). The final goal was to screen PLGA–PC NPs capable of loading large amounts of proteins (e.g. $\geq$ 20 wt % of NP) to form new polymer–protein complex NPs by utilizing the electrostatic interaction between proteins and the PLGA–PC NPs. The ideal system would require only a simple formulation method (such as mixing in aqueous solution), while the final complex NPs would retain a regular spherical shape and size < 200 nm (Figures 1 and 4). The desired structure of the new hybrid NPs would be a nucleus of PLGA–PC NPs surrounded by proteins, which primarily interact with the PC component of PLGA–PC NPs or other proteins.

First, a water-soluble L-arginine-based PC library (named PC*x*) was developed according to a modified synthesis procedure (Figure 2 and see the Supporting Information).[21,22] L-Arginine-based PCs were chosen because arginine remains positively charged in neutral, acidic, and even the most basic environments because of the high pK_a value of guanidinium groups (around 12.5), which enables the PC moiety to interact strongly with the negatively charged proteins and peptides in aqueous solutions. By setting monomer molar ratios of **I**/**II** < 1.0:1, PCs are obtained with NH_2 termini (NH_2-PC-NH_2), which are needed for further conjugation with PLGA-COOH. To engineer polymeric NPs, diblock copolymers of PLGA-*b*-PC were prepared by coupling the carboxy terminal of PLGA and the amino functionality of PC (Figure 2 and see the Supporting Information). The obtained diblock copolymers of PLGA-*b*-PC were named PLGA*y*–PC*x* (see the Supporting Information). Two types of PLGA-COOH with significantly different MWs were used: PLGA1 (M_n = 43.5 kDa) and PLGA2 (M_n = 5.0 kDa). The percentage of the PLGA–PC cationic moiety, an important factor for the protein loading functionality of the NP, could be altered by changing the PLGA MW: decreasing the PLGA MW would increase the cationic moiety density of the copolymer and the resulting NP.

The nanoprecipitation method was used to produce small, simple PLGA–PC NPs with the desired core–shell (PLGA–PC) structure. The particle size and surface charge of the PLGA–PC NPs are very important for interaction with proteins (discussed in detail below). The TEM images and DLS results (Figure 3) show that the formed PLGA–PC NPs were mostly in the range 20–80 nm, depending on the PLGA-*b*-PC composition. The PLGA MW was the dominating factor in determining the NP size: low MW PLGA2-based PLGA–PC NPs were mainly in the size range 20–40 nm (Figure 3a); while the high MW PLGA1-based PLGA–PC NPs were mainly in the size range 40–80 nm (Figure 3b). The PLGA–PC NPs were smaller than the corresponding PLGA NPs (Figure 3c). The TEM images in Figure 3a,b demonstrate that the PLGA–PC NPs were spherical or egg shaped, while the surface morphology was fluffy because of the thick PC

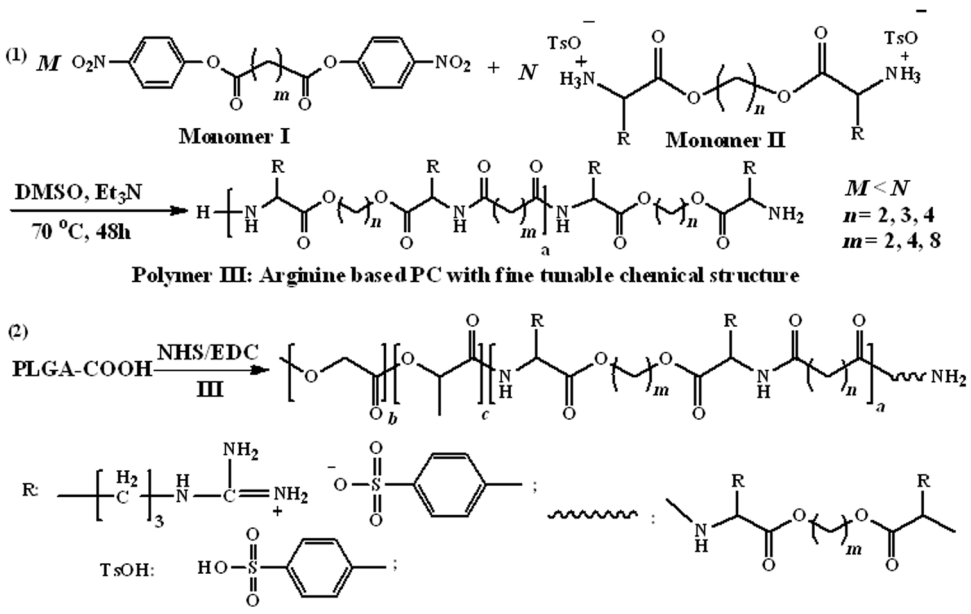

Figure 2. Synthesis of L-arginine-based PC (1) and PLGA-*b*-PC copolymer (2). Ts = *p*-toluenesulfonyl.

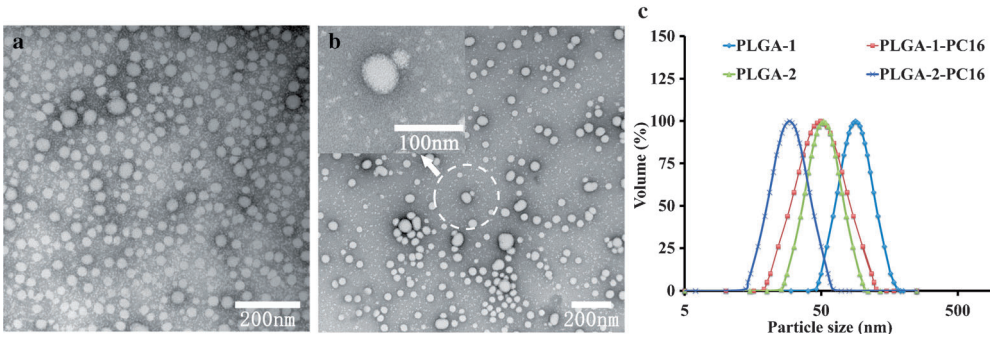

Figure 3. TEM images of PLGA–PC NPs: a) PLGA2–PC16; b) PLGA1–PC16. c) Particle size of PLGA-PC and PLGA NPs from DLS.

shell in the dried state used for TEM measurements. The zeta potential of the NPs was in the range of + 15 to 50 mV and was not correlated with the PLGA or PC structure or the MW. The cytotoxicity of the PLGA–PC NPs was evaluated with an MTT (3-(4,5-dimethylthiazol-2-yl)-2,5-diphenyltetrazolium bromide) assay, and the NPs were not toxic to either Hela or A549 cells in the concentration range of 1.0 ng mL^{-1} to 200 μg mL^{-1}.

Although many strategies have been developed for loading NPs with proteins, serious challenges remain in easily and rapidly loading a high quantity of proteins into NPs of reasonably small size in a green manner, namely, without organic solvents. The PLGA–PC NPs were designed with these goals in mind. The body charge density, not the surface charge, is believed to determine the protein-loading efficiency of a NP in this study. To better utilize the electrostatic field of the thick PC shell to strongly adsorb proteins and form new NP complexes with the desired size and protein-loading capacity, a few formulation strategies were tried until a very simple method with the lowest contamination was chosen: direct mixing of aqueous solutions containing PLGA–PC NPs and proteins. Bovine serum albumin (BSA) was used as a model protein because of its medium size (MW = 66.5 kDa) and suitable charge properties (isoelectric point = 4.7). Before the systematic study, a quick experiment was carried out to verify this proof of concept by simply mixing random amounts of PLGA–PC NP solutions with BSA solutions. Mixing produces some changes in terms of zeta potential, particle size, and structure, depending on the PLGA–PC type, weight ratio (WR) of the PLGA–PC to protein, and other formulation conditions. Figure 4a shows a TEM image obtained on mixing PLGA2–PC16 NP with 2 wt% BSA in aqueous solution as an example. After mixing, each PLGA–PC NP was loaded with some proteins on its surface. Some NPs connected through bound proteins, but the structure of this complex was random and irregular. We then wanted to investigate the relationships between protein-loading efficiency, particle size, structure, and surface charge of the PLGA–PC NP/BSA complex. We sought to determine whether we could produce PLGA–PC/BSA complexes with uniform nanostructure, small size, and high protein loading. To systematically investigate the NP–protein interaction and the structure–function relationship, two types of PLGA–PC NPs (PLGA1–PC16 and PLGA2–PC16) were selected and they had very similar structure: the PC blocks were identical, while the PLGA blocks had the same structure but significantly different MWs (43.5 kDa and 5.0 kDa, respectively). Since the MW of PC16 is around 4.5 kDa, the PC composition of PLGA1–PC16 and PLGA2–PC16 NPs are about 9.4 wt% and 47.4 wt%, respectively. Therefore, the completely different PC composition (a fivefold difference) made comparison straightforward.

For each PLGA–PC NP system, various PLGA–PC/BSA hybrid complexes were formed by simply mixing aqueous solutions with a series of desired WRs of PLGA to BSA, ranging broadly from 5000:1 to 2:1. Figure 4e,f show the particle size and zeta potential of the PLGA–PC/BSA particles as a function of the WR of PLGA–PC NP to BSA. In Figure 4e,f, the zeta potential trend can be divided into four regions. In the first region, as the WR of PLGA–PC NP to BSA decreased from 5000 to a few hundred, the zeta potential of the complex particles also decreased, which suggests that if more proteins were mixed with the PLGA–PC NPs, more of the positively charged surface of the PLGA–PC NP was surrounded or covered by negatively charged proteins through electrostatic interactions. In the second region, with more proteins added (WR from a few hundred to a few tens), almost all of the PLGA–PC NP surface was covered with proteins, and the zeta potential changed from positive to zero or slightly negative. At this stage, the corresponding WR to the 0 mV zeta potential is determined by the PC weight percentage. For the third region, a further decrease of the WR of PLGA–PC NP to protein continued to decrease the zeta potential of the complexed particle to around −30 mV. For the fourth region, the zeta potential continued to decrease or formed a plateau at a value slightly more negative than the zeta potential of pure BSA. The particle size trend in Figure 4e,f can also be divided into the same four regions. In the first region, as the WR of PLGA–PC to BSA decreased, the size of the complex particle slightly and steadily increased, which suggests that as more protein was added into the PLGA–PC NP solutions, the PLGA–PC NPs began to adsorb more proteins on their surface. In the second region, as the WR of PLGA–PC NP to protein decreased further, the particle size of the PLGA–PC NP/protein complexes significantly increased beyond the expected size range, thus indicating some form of connections with the NPs. For the largest particle size obtained in this region, the corresponding zeta potential was around zero. After the second region, however, a continuing decrease of the WR in a narrow range (third region) immediately resulted in a significant reduction of the size of the complex particle. This phenomenon suggests that the PLGA–PC NP/protein complex particle may be stable within this narrow WR range and is likely the optimal formulation. One possible reason for

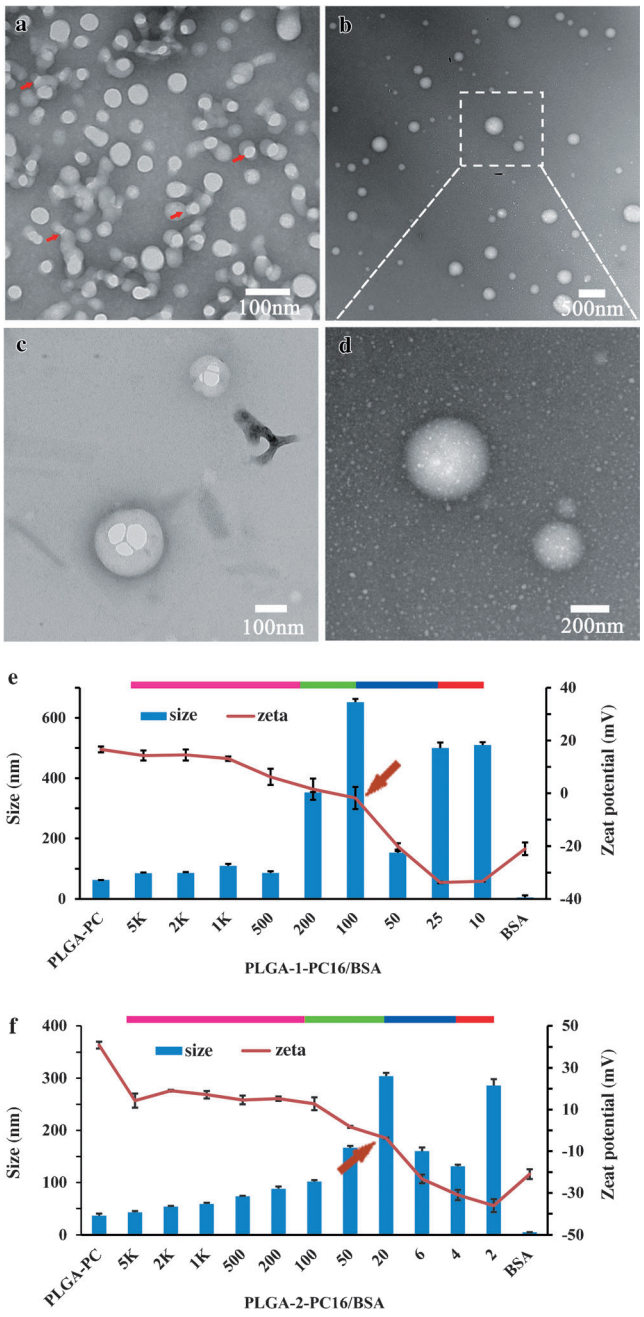

Figure 4. TEM images of PLGA–PC/protein nanoparticles (a–d): a) PLGA2-PC 16 with 2 wt% BSA loading; b–d) PLGA2–PC16 with 25 wt% BSA loading. Structure–function relationship between the zeta potential, particle size, and weight ratio of the PLGA–PC/BSA complex particle (e,f).

this stable state is that the total positive charge of the PLGA–PC NPs is equal to or close to the total negative charge of the BSA molecules. The small particle size had a corresponding zeta potential of approximately −20 mV. In this region, the PLGA2–PC16 NPs had loaded protein in the range 15–30 wt% with encapsulation efficiency over 95%. However, for the PLGA1–PC16 NPs, the corresponding protein-loading region was in the range 2–3 wt% as a result of the low PC density, but with similar encapsulation efficiency. In the fourth region, the continuously decreasing WR caused significant particle size increases, which indicates a lack of stable complexes and heavy aggregation at the higher WR of BSA to PLGA–PC NPs. These results show that for each type of PLGA–PC16 NP, the maximum effective loading efficiency was achieved at a small particle size with a zeta potential range of −10 to −30 mV, in a specific and narrow WR range of PLGA–PC to BSA. Figure 4e,f show the same trends for both size and zeta potential, but different corresponding WR windows for the specific small particle size, thus suggesting that this is a function of the polymer structure. These relationships hold true for all the other developed PLGA–PC NPs. Briefly, PLGA2–PC NPs have around 10 times the BSA loading capability of the corresponding PLGA1–PC NPs, and the highest BSA loading with small particle size always happened in a narrow WR range. When the order of addition was changed (nanoparticle solution was added into BSA), the complexed particles were larger in the third region.

Based on the above findings regarding zeta potential and particle size, our findings in the third region of the PLGA2–PC system were highly interesting: the complexed particles had small sizes but maintained significant protein loading. TEM was used to study the complexed particle structure in this region for the PLGA2–PC system. To acquire better image quality and resolve more details, the formulation procedure was slightly modified (see the Supporting Information) so that NPs with larger size could be obtained without affecting the structure. Figure 4b shows PLGA2–PC/BSA NPs with relatively large sizes at a WR of 4. It was surprising to find that all of the new NPs formed by simple mixing were uniform and spherical complexed NPs. Figure 4d shows a magnified image of two such nanospheres from Figure 4b. The structure and surface morphology of the complexed NPs were different from that of the pure PLGA–PC NPs in Figure 3. On the basis of the NP size and protein loading amount, it was predicted that multiple PLGA–PC NPs would be contained in a single complex NP (size $\geq$80 nm). Through TEM, the inner structure of some NP complexes was examined, thereby confirming multiple PLGA–PC NPs inside, acting as nucleus. Figure 4c shows an example of complexed PLGA2–PC16/BSA, with the size of the internal, smaller PLGA2–PC16 NPs consistent with those in Figure 3a.

Other proteins/peptides, including ovalbumin, TNF-α, insulin, and Ac2-26 peptide, were evaluated for interaction with PLGA–PC NPs. The results and relationships were similar to those found above: complex nanoparticles were formed with PLGA2–PC16 at $\geq$20 wt% loading and $\leq$200 nm size. The MWs of proteins/peptides did not significantly affect interactions between the PLGA–PC NPs and proteins. Additionally, multiple types of proteins could be loaded simultaneously without making apparent sacrifices in loading efficiency of each protein (see the Supporting Information). The in vitro and in vivo bioactivity of loaded proteins was evaluated by testing the released TNF-α and insulin, respectively. The results indicated that this loading strategy did not significantly affect the bioactivity of released proteins (see the Supporting Information). Other types of PLGA-*b*-PCs with similar MWs and PLGA composition were developed for comparison. NPs of <50–60 nm formed, but

they could not effectively load large amounts of proteins (see the Supporting Information).

The specific complexed PLGA2–PC16/protein nanospheres formed in the third region were unstable in buffered solutions. After optimization, it was found that lipid/lipid–PEG (such as DSPE–PEG(MW≥2000)) effectively stabilized the negatively charged nanospheres without causing any apparent size change, with only a 5–10 wt% loss in overall protein loading (see the Supporting Information). The stabilization could be due to self-assembly of cationic and hydrophobic lipid/lipid–PEG on the surface of PLGA2–PC16/protein nanospheres, which was confirmed by TEM, the changes in the particle size and surface charge, and small protein loss. Figure 5a shows a TEM image of a PLGA2–PC/protein nanosphere coated with DSPE–PEG3000/lecithin. Study of the release profile of these nanospheres in PBS buffer (Figure 5b) revealed some burst release (around 25 wt%) after coating with lipid–PEG and addition of buffers. Fast release occurred over the first 1–2 days, especially in the initial hours. After that, the release of BSA was sustained and steady for at least three weeks. Finally, BSA molecules labeled with red fluorescent dye RITC were loaded to study the cellular interaction of the PLGA2–PC/protein nanospheres (see the Supporting Information). Figure 5c,d show the cellular uptake of pure RITC–BSA compared to the complex of PLGA2–PC NP/RITC–BSA/DSPE–PEG3000 after four hours of incubation. After four hours, large numbers of NPs entered the cells, and the proteins began to be released in a sustained fashion.

In summary, a new PLGA–PC NP platform with a core–shell structure and a new "green" protein-loading strategy were developed and evaluated for protein delivery as well as structure–function relationships. Two issues were investigated: 1) the effect of the PLGA–PC structure on the resulting NP structure and protein encapsulation capability, and 2) the relationship between the size of the PLGA–PC/protein NPs, their zeta potential, and protein-loading efficiency. The results indicated that the PLGA–PC polymer structure primarily dictates the NP size and interaction with proteins. The particle size, zeta potential, and weight ratio of the PLGA–PC NP/protein are also closely related. Some screened PLGA–PC NPs were able to interact with proteins, thereby forming new multinuclear spherical NPs with high protein loading (20–40 wt%) and 100–200 nm size by simple mixing in aqueous solutions. These findings could facilitate the development of new robust protein-delivery platforms or the modification of currently existing platforms for green protein loading.

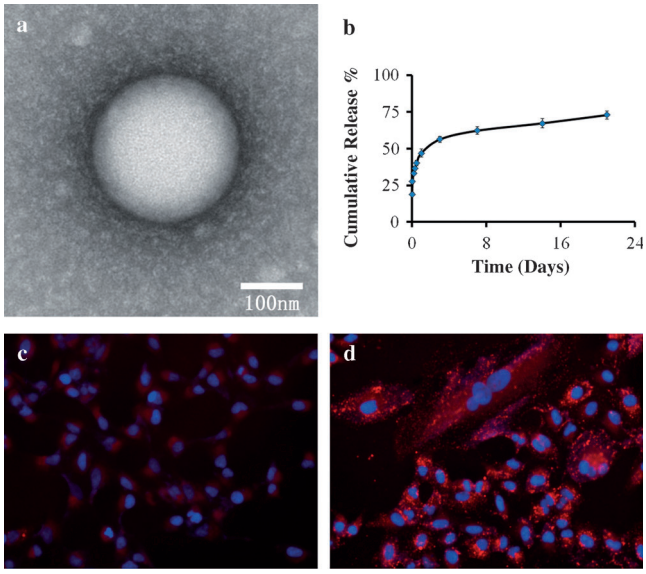

Figure 5. a) and b) TEM image and release profile of PLGA2-PC16 NP/BSA/DSPE-PEG3000; c) and d) the cellular uptake of fluorescence BSA (c) and PLGA2-PC16 NP/fluorescence BSA/DSPE-PEG3000 (d) after 4 h. DSPE = 1,2-distearoyl-sn-glycero-3-phosphoethanolamine.

Received: April 28, 2014
Published online: July 2, 2014

Keywords: nanoparticles · polycations · polymers · protein delivery · structure–function relationships

[1] R. Langer, D. A. Tirrell, *Nature* **2004**, *428*, 487.
[2] Z. Gu, A. Biswas, M. Zhao, Y. Tang, *Chem. Soc. Rev.* **2011**, *40*, 3638.
[3] T. Vermonden, R. Censi, W. E. Hennink, *Chem. Rev.* **2012**, *112*, 2853.
[4] N. Kamaly, G. Fredman, M. Subramanian, S. Gadde, A. Pesic, L. Cheung, Z. A. Fayad, R. Langer, I. Tabas, O. Cameron Farokhzad, *Proc. Natl. Acad. Sci. USA* **2013**, *110*, 6506.
[5] M. Yan, J. Du, Z. Gu, M. Liang, Y. Hu, W. Zhang, S. Priceman, L. Wu, Z. H. Zhou, Z. Liu, T. Segura, Y. Tang, Y. Lu, *Nat. Nanotechnol.* **2010**, *5*, 48.
[6] E. M. Pridgen, F. Alexis, T. T. Kuo, E. Levy-Nissenbaum, R. Karnik, R. S. Blumberg, R. Langer, O. C. Farokhzad, *Sci. Transl. Med.* **2013**, *5*, 213ra167.
[7] H. C. Kang, J. E. Lee, Y. H. Bae, *J. Controlled Release* **2012**, *160*, 440.
[8] N. A. Peppas, K. M. Wood, J. O. Blanchette, *Expert Opin. Biol. Ther.* **2004**, *4*, 881.
[9] W. Yan, L. Huang, *Polym. Rev.* **2007**, *47*, 329.
[10] R. Duncan, *Nat. Rev. Drug Discovery* **2003**, *2*, 347.
[11] S. Brahmachari, D. Das, A. Shome, P. K. Das, *Angew. Chem.* **2011**, *123*, 11439; *Angew. Chem. Int. Ed.* **2011**, *50*, 11243.
[12] H. Ayame, N. Morimoto, K. Akiyoshi, *Bioconjugate Chem.* **2008**, *19*, 882.
[13] N. Kamaly, Z. Xiao, P. M. Valencia, A. F. Radovic-Moreno, O. C. Farokhzad, *Chem. Soc. Rev.* **2012**, *41*, 2971.
[14] J. Shi, Z. Xiao, N. Kamaly, O. C. Farokhzad, *Acc. Chem. Res.* **2011**, *44*, 1123.
[15] N. Bertrand, J. Wu, X. Xu, N. Kamaly, O. C. Farokhzad, *Adv. Drug Delivery Rev.* **2014**, *66*, 2.
[16] T. G. Park, W. Lu, G. Crotts, *J. Controlled Release* **1995**, *33*, 211.
[17] B. S. Zolnik, D. J. Burgess, *J. Controlled Release* **2008**, *127*, 137.
[18] O. C. Farokhzad, S. Jon, A. Khademhosseini, T.-N. T. Tran, D. A. LaVan, R. Langer, *Cancer Res.* **2004**, *64*, 7668.
[19] J. Shi, Z. Xiao, A. R. Votruba, C. Vilos, O. C. Farokhzad, *Angew. Chem.* **2011**, *123*, 7165; *Angew. Chem. Int. Ed.* **2011**, *50*, 7027.
[20] L. Zhang, J. M. Chan, F. X. Gu, J.-W. Rhee, A. Z. Wang, A. F. Radovic-Moreno, F. Alexis, R. Langer, O. C. Farokhzad, *ACS Nano* **2008**, *2*, 1696.
[21] J. Wu, D. Wu, M. A. Mutschler, C.-C. Chu, *Adv. Funct. Mater.* **2012**, *22*, 3815.
[22] J. Wu, D. Yamanouchi, B. Liu, C.-C. Chu, *J. Mater. Chem.* **2012**, *22*, 18983.

